Flexible Body Dynamic Stability for High Performance Aircraft

N91-22318

By

E. A. Goforth*, H. M. Youssef**, C. V. Apelian†, S. C. Schroeder††
Lockheed Aeronautical Systems Company
P.O.Box 551
Burbank, CA 91520-7550

ABSTRACT

Dynamic equations which include the effects of unsteady aerodynamic forces and a flexible body structure have been developed for a free-flying high performance fighter aircraft. The linear and angular deformations are assumed to be small in the body reference frame, allowing the equations to be linearized in the deformation variables. Equations for total body dynamics and flexible body dynamics are formulated using the hybrid coordinate method and integrated in a state space format. A detailed finite element model of a generic high-performance fighter aircraft is used to generate the mass and stiffness matrices. Unsteady aerodynamics are represented by a rational function approximation of the doublet lattice matrices. The equations simplify for the case of constant angular rate of the body reference frame, allowing the effect of roll rate to be studied by computing the eigenvalues of the system. It is found that the rigid body modes of the aircraft are greatly affected by introducing a constant roll rate, while the effect on the flexible modes is minimal for this configuration.

1. INTRODUCTION

Future fighter aircraft must be able to meet stringent maneuverability and performance requirements. This will result in aircraft designs in which the interaction of flexibility, aerodynamics, and overall body motion during a maneuver are of prime importance. The need for superagility and the use of advanced lightweight materials will make it very important to consider flexibility effects in the analysis of the aircraft undergoing maneuvers at high rates.

Flexible body dynamics have been investigated in many other writings, including references [1] - [4]. In this paper, dynamic equations will be derived in a manner similar to that in reference [5], which contains a more thorough development of the equations. In addition, aerodynamic forces will be explicitly included in the equations. These equations will then be applied to a realistic model of a modern fighter aircraft.

The aircraft is assumed to be a collection of elastically interconnected, discrete rigid subbodies which are subjected to external forces and torques, including unsteady aerodynamic forces. It is assumed that the deformations of the subbodies with respect to the body reference frame are small so that the high order terms in the deformation variables and their rates can be neglected. The rotational effects of motors, fans, and turbines are not included in this representation.

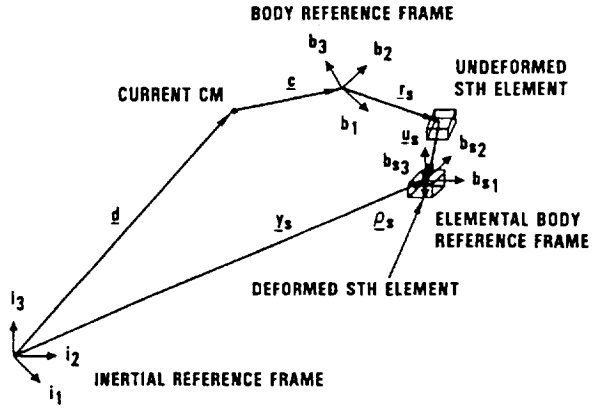

Figure 1. Reference Frames and a Subbody

*Senior Research Specialist
**Department Engineer
†Associate Engineer
††Senior Associate Engineer

Table 1. Vectors and Dyads definitions

Vectors and Dyads	Definition
$\{i\}^T$	basis matrix for inertial reference frame (IRF)
$\{b\}^T$	basis matrix for body reference frame (BRF)
$\{i\}^T = \{b\}^T \theta$	direction cosine matrix relationship between IRF and BRF
$\omega = \{b\}^T \omega$	angular velocity of body reference frame
$\{b_s\}^T$	basis matrix for sth elemental body reference frame(ERF)
$\underline{d} = \{i\}^T d$	Position of current center of mass (CM) in IRF
$\underline{V} = \{i\}^T V$	Velocity of current CM in IRF
$\underline{Y}_s = \{i\}^T Y_s$	Position of the sth element in IRF
$\underline{c} = \{b\}^T c$	position of CM in BRF
$\underline{r}_s = \{b\}^T r_s$	position of undeformed sth element from undeformed CM
$\underline{u}_s = \{b\}^T u_s$	position of sth element from the undeformed position
$\underline{\rho}_s = \{b_s\}^T \rho_s$	position of differential mass in sth elemental body
$\underline{\beta}_s = \{b\}^T \beta_s$	angular deformation of sth element
$\underline{\underline{I}} = \{b\}^T I \{b\}$	Inertia dyadic of the aircraft with respect to CM
$\underline{\underline{I}}_s = \{b_s\}^T I_s \{b_s\}$	Inertia dyadic of the sth elemental body about its CM

Table 2. Vector Identities and Matrix Operation Equivalents

Vector representation:

$$\underline{x} = \{i\}^T \begin{bmatrix} x1 \\ x_2 \\ x_3 \end{bmatrix} = \{i\}^T X$$

$$\underline{y} = \{i\}^T \begin{bmatrix} y_1 \\ y_2 \\ y_3 \end{bmatrix} = \{i\}^T Y$$

Cross product representation:

$$\underline{x} \times \underline{y} = \{i\}^T \tilde{X} Y = - \{i\}^T \tilde{Y} X$$

where the $\tilde{}$ operator is defined below:

$$(X)\tilde{} = \tilde{X} = \begin{bmatrix} 0 & -x_3 & x_2 \\ x_3 & 0 & -x_1 \\ -x_2 & x_1 & 0 \end{bmatrix}$$

Operations with dyad

$$\underline{\underline{I}} = \{i\}^T I \{i\}$$

$$\underline{\underline{I}} \cdot \underline{x} = \{i\}^T I X$$

$$\underline{\underline{I}} \times \underline{x} \cdot \underline{y} = \{i\}^T I \tilde{X} Y$$

A highly detailed description of the hybrid coordinate method, which is used here to develop the dynamic equations, can be found in references [5] and [6]. Only some highlights of the development of these equations will be presented in this paper. The development of the equations closely follows that of reference [7], with aerodynamic forces added. The equations are implemented as a computer program, FLXAIR.

Figure 1 shows a schematic diagram of the various reference frames associated with each subbody. Definitions of the vectors and dyads used in this figure and in the derivations are given in Table 1. Table 2 shows the equivalency between various operations in a vector/dyad format and those in a matrix format. The matrix format is used for implementing the computer solution to our problem.

Section 2 deals with the net force and torque applied to the total body. The net forces and torques on the subbodies are described in section 3. Derivations are kept brief, with only main steps provided. The rational function approximation used for describing the unsteady aerodynamic forces is given in section 4. In section 5 the equations are integrated in a state space format, with aerodynamic forces specifically separated from other external forces. These nonlinear and time dependent equations can be used for simulation. When the angular velocity of the body reference frame is constant, the equations become time invariant. It is then possible to study the effects of angular velocity on vehicle structural dynamics by performing an eigenvalue analysis. When unsteady aerodynamic loading is included in this formulation, this is seen to be a flutter analysis under maneuver.

A large-order finite element model which is a realistic representation of an advanced fighter was used to demonstrate the stability effects of high roll rates. Section 6 describes the NASTRAN

model, structural and aerodynamic, which was used in the analysis. Results are shown for various roll rates and for variations of overall stiffness of the aircraft. The analyses show little effect on the flexible modes of the system due to roll maneuvers. Considerable effect was, however, observed for the rigid body modes.

2. TOTAL BODY DYNAMICS

The equations are derived from Newton-Euler equations. The equations for the net force $\underline{F}$, and the net torque $\underline{P}$, can be represented as follows.

$$\underline{F} = {}^{i}\frac{d^2}{dt^2}(M_{Tot}\,\underline{d}) \tag{1}$$

$$\underline{P} = {}^{i}\frac{d}{dt}(\underline{H}) \tag{2}$$

M_{Tot} is the total mass, and $\underline{H}$ is the angular momentum referred to the CM of the aircraft. Presuperscript i refers to the fact that the differentiation must be with respect to the inertial reference frame.

The further development neglects the effects of rotating bodies such as engine compressors, fans, rotors, etc.. It is assumed that the deformation of flexible bodies is small in the body reference frame. This assumption is used to neglect the high order terms in the deformation variables $\underline{u}_s$(linear deformation of sth element) and $\underline{\beta}_s$(angular deformation of the sth element) and their derivatives.

Equation (1) can be written in the body reference frame and for ease of computer implementation in matrix form as follows:

$$F = M_{Tot}\,\dot{V} \tag{3}$$

The development of equation (2) to a computer implementable step is lengthy. Only fev key steps are given.
The angular momentum $\underline{H}$ is defined as

$$\underline{H} = \int(\underline{c}+\underline{r}_s+\underline{u}_s+\underline{\rho}_s) \times {}^{i}\frac{d}{dt}(\underline{c}+\underline{r}_s+\underline{u}_s+\underline{\rho}_s)\,dm \tag{4}$$

The development makes use of the mass-center definition

$$\int(\underline{c}+\underline{r}_s+\underline{u}_s+\underline{\rho}_s)\,dm = 0 \tag{5}$$

and the following identity:

$$\int(\underline{r}_s+\underline{u}_s+\underline{\rho}_s) \times (\underline{\omega} \times (\underline{r}_s+\underline{u}_s+\underline{\rho}_s))\,dm = \underline{\underline{I}} \cdot \underline{\omega} \tag{6}$$

With the use of equations (4) to (6), equation (2) can be written as

$$\underline{P} = \underline{\underline{I}}\cdot\dot{\underline{\omega}} + \underline{\omega} \times \underline{\underline{I}} \cdot \underline{\omega} + \dot{\underline{\underline{I}}}\cdot\underline{\omega} + \ddot{\underline{c}} \times \underline{c} + {}^{i}\frac{d}{dt}\int(\underline{r}_s+\underline{u}_s+\underline{\rho}_s) \times (\dot{\underline{r}}_s+\dot{\underline{u}}_s+\dot{\underline{\rho}}_s)\,dm \tag{7}$$

The assumptions of discrete lumped masses and small deformations with respect to the body reference frame are now used to convert the integration operation into the following summation operation:

$$\int(\underline{r}_s+\underline{u}_s+\underline{\rho}_s) \times (\dot{\underline{r}}_s+\dot{\underline{u}}_s+\dot{\underline{\rho}}_s)\,dm = \Sigma \underline{r}_s \times m_s\,\dot{\underline{u}}_s + \Sigma\,\underline{\underline{I}}_s \cdot \dot{\underline{\beta}}_s \tag{8}$$

where m_s is defined as:

$$\int_s dm = m_s \tag{9}$$

and center of mass definition of sth lumped mass is given by

$$\int_s \underline{\rho}_s\,dm = 0 \tag{10}$$

Finally, equation (7) can be written in a computer implementable form as:

$$P = I\dot{\omega} + \dot{I}\omega + \tilde{\omega}I\omega + \Sigma[((\tilde{\omega}r_s)^{\sim} + \tilde{r}_s\tilde{\omega})\dot{u}_s m_s + \tilde{r}_s\ddot{u}_s m_s + I_s\ddot{\beta}_s] + \tilde{\omega}\Sigma I_s\dot{\beta}_s \tag{11}$$

The total inertia is assumed to be linear in the deformation variables.

$$I = I^* + \Sigma m_s\{2r_s^T u_s E - r_s u_s^T - u_s r_s^T\} + \Sigma(\tilde{\beta}_s I_s - I_s\tilde{\beta}_s) \tag{12}$$

where I^* is the inertia of the undeformed airplane. Therefore

$$\dot{I} = \Sigma m_s\{2r_s^T\dot{u}_s E - r_s\dot{u}_s^T - u_s\dot{r}_s^T\} + \Sigma(\dot{\tilde{\beta}}_s I_s - I_s\dot{\tilde{\beta}}_s) \tag{13}$$

Equations (12) and (13) can be substituted into equation (11) to further simplify the equation.

3. ELEMENTAL BODY DYNAMICS

The net forces and torques on the sth elemental body are as follows:

$$\underline{f}_s = m_s \, {}^i\frac{d^2}{dt^2}(\underline{d} + \underline{c} + \underline{r}_s + \underline{u}_s) \tag{14}$$

$$\underline{p}_s = {}^i\frac{d}{dt}\underline{H}_s \tag{15}$$

$\underline{H}_s$ is the inertial angular momentum of sth element referred to its mass center. Note that this equation is applicable to all n subbodies.

It is assumed that the body reference frame and the elemental body reference frames are initially colinear. This assumption, though not necessary, is used here to simplify the equations.

Equation (14) can be written in the following computer implementable form:

$$f_s = m_s \{ \theta\dot{V} + \ddot{c} + \dot{\tilde{\omega}}(r_s+u_s+c) + 2\tilde{\omega}(\dot{c}+\dot{u}_s) + \ddot{u}_s + \tilde{\omega}\tilde{\omega}(r_s+u_s+c) \} \tag{16}$$

noting that

$$V = \frac{d}{dt}(d) \tag{17}$$

$\underline{H}_s$ is defined as

$$\underline{H}_s = \underline{I}_s \cdot \underline{\omega} \tag{18}$$

Invoking the assumption of small deformation, the rotation is represented by

$$\underline{\beta}_s = \{b\}^T \beta_s \tag{19}$$

Note that this equation is strictly true if the rotations are infinitesimally small. The relationship between the body reference frame and the elemental reference frame can now be approximated as

$$\{b_s\}^T = \{b\}^T (E+\tilde{\beta}_s) \tag{20}$$

where E is a 3x3 unit matrix.

Using equations (18) to (20), equation (15) can be written in the following computer implementable form:

$$p_s = I_s(\dot{\omega}+\ddot{\beta}_s) + (I_s\tilde{\omega}+\tilde{\omega}I_s-(I_s\omega)^{\sim})\dot{\beta}_s + \tilde{\omega}I_s\omega + (I_s\dot{\tilde{\omega}} - (I_s\dot{\omega})^{\sim} - \tilde{\omega}(I_s\omega)^{\sim} + \tilde{\omega}I_s\tilde{\omega})\beta_s \tag{21}$$

4. RATIONAL FUNCTION APPROXIMATION OF UNSTEADY AERODYNAMICS

The formulation of the unsteady aerodynamics is based on the relation

$$\{\frac{w}{V}\} = \frac{2}{\rho V^2} [NID] \{\Delta p\} \tag{22}$$

where $\{\Delta p\}$ represents the pressures at aerodynamic force nodes, $\{w\}$ contains the velocities normal to the lifting surface induced by $\{\Delta p\}$, and [NID] is the induced normal downwash influence matrix. The induced velocities are defined as downwash collocation points which are located at the 3/4 chord of each aerodynamic box for the doublet lattice method.

Downwash collocation points are those points on a lifting surface at which the induced velocity normalized by the free stream velocity is equal to the local angle of attack $\{a\}$, i.e.,

$$\{a\} = \{\frac{w}{V}\} \tag{23}$$

The pressures are then given by

$$\{\Delta p\} = \frac{1}{2} \rho V^2 [NID]^{-1} \{a\} \tag{24}$$

or

$$\{\Delta p\} = \frac{1}{2} \rho V^2 [AIC] \{a\} \tag{25}$$

where $[AIC] = [NID]^{-1}$.

In the following derivation, Equation (24) is used as a starting point.

From $\{\Delta p\}$, by an integration or "lumping" process represented by [ZP], the aerodynamic forces are obtained:

$$\{Z_{aero}\} = [ZP] \{\Delta p\} \tag{26}$$

The local angle of attack, taken relative to the free stream velocity, V, is given by

$$\{a\} = \{a_T\} + \{a_z\} \tag{27}$$

The contribution a_T is the instantaneous slope of the lifting surface, relative to V, in a plane through V perpendicular to the lifting

surface:

$$\{a_T\} = [D_\theta]\{z\} \tag{28a}$$

where $[D_\theta]$ is a differentiating matrix.

The contribution $a_{\dot{z}}$ results from the rate of translation in a direction perpendicular to the lifting surface:

$$\{a_{\dot{z}}\} = [D_z]\left\{\frac{\dot{z}}{V}\right\} \tag{28b}$$

where $[D_z]$ is an interpolating matrix.

Substituting Equation (28) into Equation (27) and replacing $\dot{z}$ by sz yields:

$$\{a\} = \left[[D_\theta] + \frac{s}{V}[D_z]\right]\{z\} \tag{29}$$

Combining Equations (24), (26) and (29) leads to:

$$\{Z_{aero}\} = \frac{1}{2}\rho V^2[ZP][NID]^{-1} * \left[[D_\theta] + \frac{s}{V}[D_z]\right]\{z\} \tag{30}$$

For constant amplitude oscillation $s = i\omega = i(Vk/c)$. The induced velocity matrix is a function of ik. It follows that Equation (30) can be written as:

$$\{Z_{aero}\} = \frac{1}{2}\rho V^2[A(ik)]\{z\} \tag{31}$$

where A(ik) is given by:

$$[A(ik)] = [ZP][NID(ik)]^{-1}\left[[D_\theta] + \frac{ik}{c}[D_z]\right] \tag{32}$$

For developing the explicit function of s, $[A(s)]$, corresponding to $[A(ik)]$, the $[D_\theta]$ and $[D_z]$ contribution to $[A(ik)]$ are identified separately, and the explicit occurrence of s in Equation (30) is maintained.

$$[A(ik,s)] = [ZP][NID(ik)]^{-1} * [D_\theta] + \frac{s}{V}[ZP][NID(ik)]^{-1}[D_z] \tag{33}$$

Let:

$$[A_T(ik)] = [ZP][NID(ik)]^{-1}[D_\theta] \tag{34}$$

and

$$[A_z(ik)] = [Zp][NID(ik)]^{-1}[D_z] \tag{35}$$

Then:

$$[A(ik,s)] = [A_T(ik)] + \frac{s}{V}[A_z(ik)] \tag{36}$$

Preliminary to approximating $[A(ik,s)]$ by an explicit function of only s, $[A_T(ik)]$ and $[A_z(ik)]$ are approximated by $[A_T(p)]$ and $[A_z(p)]$, where p is the nondimensional form of s: $p = cs/V$.

Following Reference [8], the following terms are approximately,

$$[A_T(p)] = [B_{T0}] + \sum_{j=1}^{n}\frac{[B_{Tj}]p}{p + b_j} \tag{37}$$

$$[A_z(p)] = [B_{z0}] + \sum_{j=1}^{n}\frac{[B_{zi}]p}{p + b_j} \tag{38}$$

These matrices can be obtained by generating aerodynamic matrices for several values of k and then employing a least-squares fit.

Because the state-space equation will be written in terms of s, Equations (37) and (38) are written in terms of s by letting $p = cs/V$:

$$[A_T(s)] = [B_{T0}] + s\sum_{j=1}^{n}\frac{[B_{Tj}]}{s + \beta_j} \tag{39}$$

$$[A_z(s)] = [B_{z0}] + s\sum_{j=1}^{n}\frac{[B_{zj}]}{s + \beta_j} \tag{40}$$

where

$$\beta_j = V b_j/c$$

Combination of Equations (31), (35), (36), (39), and (40) leads to the following approximate expressions for the aerodynamic forces:

$$\{Z_{aero}\} = \frac{1}{2}\rho V^2\left[[B_{T0}] + s\sum_{j=1}^{n}\frac{[B_{Tj}]}{s + \beta_j}\right]\{z\} + \frac{1}{2}\rho V^2\left[\frac{s}{V}[B_{z0}] + \frac{s^2}{V}\sum_{j=1}^{n}\frac{[B_{zj}]}{s + \beta_j}\right]\{z\} \tag{41}$$

5. INTEGRATED TOTAL BODY AND ELEMENTAL BODY DYNAMICS

The general form of the linear flexible body equation is

$$M'\ddot{q} + D\dot{q} + G'(\tilde{\omega})\dot{q} + K'(\tilde{\omega}\tilde{\omega},K)q + A'(\dot{\tilde{\omega}},\tilde{\omega})q = L'(\dot{\tilde{\omega}},\tilde{\omega},f_s,p_s) \quad (42)$$

where $q=[u_1^T,\beta_1^T,..,u_s^T,\beta_s^T,..,u_n^T,\beta_n^T]^T$. M, D, and K are mass, damping, and stiffness matrices respectively of the airplane which are obtained by a traditional finite element method, such as NASTRAN. The other terms, G', K', A' and L' are obtained from equations (16), and (42). Note that K' is a symmetric matrix. Equations (3), (11), (12), (13) and (42) can be written in the state space like format as follows:

$$\begin{bmatrix} M_{Tot}\theta & 0 & 0 & 0 \\ 0 & I^* & 0 & \Gamma_0 \\ 0 & 0 & E_n & 0 \\ M\Sigma_{E0}\theta & \Lambda_0 & 0 & M' \end{bmatrix} \begin{bmatrix} \dot{V} \\ \dot{\omega} \\ \dot{\eta}_1 \\ \dot{\eta}_2 \end{bmatrix} + \begin{bmatrix} 0 & 0 & 0 & 0 \\ 0 & \tilde{\omega}I^* & \bar{\Sigma} & \Gamma_1 \\ 0 & 0 & 0 & -E_n \\ 0 & \Lambda_1 & K'+A' & G'+D \end{bmatrix} \begin{bmatrix} V \\ \omega \\ \eta_1 \\ \eta_2 \end{bmatrix} = \begin{bmatrix} F \\ P \\ 0 \\ \lambda \end{bmatrix} \quad (43)$$

Equations (44)-(55) explain various terms in equation (43).

$$\eta_1 = q \quad (44)$$

$$\eta_2 = \dot{q} \quad (45)$$

0 is a null matrix and dimensions are context dependent.

E_n is 6nx6n matrix.

$$\Gamma_0\dot{\eta}_2 = \Sigma m_s r_s \ddot{u}_s + \Sigma I_s \ddot{\beta}_s \quad (46)$$

$$\Sigma\dot{\eta}_1 = \tilde{\omega}\{\Sigma m_s(2r_s^T u_s E - r_s u_s^T - u_s r_s^T) + \Sigma\tilde{\beta}_s I_s - \Sigma I_s\tilde{\beta}_s\}\omega + \{\Sigma m_s(2r_s^T u_s E - r_s u_s^T - u_s r_s^T) + \Sigma\tilde{\beta}_s I_s - \Sigma I_s\tilde{\beta}_s\}\omega \quad (47)$$

$$\Gamma_1\eta_2 = \{\Sigma m_s(2r_s^T\dot{u}_s E - r_s\dot{u}_s^T - \dot{u}_s r_s^T) + \Sigma\dot{\tilde{\beta}}_s I_s - \Sigma I_s\dot{\tilde{\beta}}_s\}\omega + \Sigma m_s[(\tilde{\omega}r_s)^\sim + \tilde{r}_s\tilde{\omega}]u_s + \Sigma\tilde{\omega}I_s\beta_s \quad (48)$$

E = 3x3 unit matrix

M = block diagonal 6nx6n matrix where block diagonals are 3x3 matrices

= Block diagonal [m_1E, I_1, .., m_sE, I_s, .., m_nE, I_n]

Σ_{E0} = [E 0 E 0 .. E 0]^T 6nx3 matrix

Σ_{0E} = [0 E 0 E .. 0 E]^T 6nx3 matrix

$$M' = M(E_n - \Sigma_{E0}\Sigma^T_{E0}M/M_{Tot}) \quad (49)$$

$$\Lambda_0 = M(\Sigma_{0E} - \tilde{R}) \quad (50)$$

$$\tilde{R} = \begin{bmatrix} \tilde{r}_1 \\ 0 \\ \tilde{r}_2 \\ 0 \\ \vdots \\ \tilde{r}_n \\ 0 \end{bmatrix} \quad (51)$$

$$\Lambda_1 = [\Sigma_{0E}\omega]^\sim M\Sigma_{0E} - M[\Sigma_{E0}\omega]^\sim\tilde{R} \quad (52)$$

$[\Sigma_{0E}\omega]^\sim$ = block diagonal matrix of dimension 6nx6n. Each block is 3x3.
The diagonal blocks are
[$\tilde{\omega}$ 0 $\tilde{\omega}$ 0 .. $\tilde{\omega}$ 0]

$[\Sigma_{E0}\omega]^\sim$ = block diagonal matrix of dimension 6nx6n. Each block is 3x3.
The diagonal blocks are
[0 $\tilde{\omega}$ 0 $\tilde{\omega}$ .. 0 $\tilde{\omega}$]

$[M\Sigma_{0E}\omega]^\sim$ = block diagonal matrix of dimension 6nx6n. Each block is 3x3.
The diagonal blocks are
[0 $(I_1\omega)^\sim$ 0 $(I_2\omega)^\sim$ .. 0 $(I_n\omega)^\sim$]

$$K' = K + [\Sigma_{0E}\omega]^\sim M[\Sigma_{0E}\omega]^\sim + M\{[\Sigma_{E0}\omega]^\sim[\Sigma_{E0}\omega]^\sim - \Sigma_{E0}\tilde{\omega}\tilde{\omega}\Sigma^T_{E0}M/M_{Tot}\} \quad (53)$$

$$A' = M[\Sigma_{OE}\dot{\omega}]^{\sim} - [M\Sigma_{OE}\dot{\omega}]^{\sim} + M\{[\Sigma_{EO}\dot{\omega}]^{\sim} - \Sigma_{EO}\dot{\bar{\omega}}\Sigma_{EO}M/M_{Tot}\} + [\Sigma_{OE}\omega]^{\sim}[M\Sigma_{OE}\omega]^{\sim} \quad (54)$$

$$G' = M[\Sigma_{OE}\omega]^{\sim} + [\Sigma_{OE}\omega]^{\sim}M - [M\Sigma_{OE}\omega]^{\sim} + 2M\{[\Sigma_{EO}\omega]^{\sim} - \Sigma_{EO}\bar{\omega}\Sigma_{EO}M/M_{Tot}\} \quad (55)$$

Definitions of $[\Sigma_{OE}\dot{\omega}]^{\sim}$, $[\Sigma_{EO}\dot{\omega}]^{\sim}$, and $[M\Sigma_{OE}\dot{\omega}]^{\sim}$ are very similar to $[\Sigma_{OE}\omega]^{\sim}$, $[\Sigma_{EO}\omega]^{\sim}$, and $[M\Sigma_{OE}\omega]^{\sim}$ and hence they are not given here.

Equation (43) has the form

$$A_0\dot{X} + A_1 X = U \quad (56)$$

where definitions of A_0, A_1, X, and U are obvious. Equation (56) can be written as

$$\dot{X} = -A_0^{-1}A_1 X + A_0^{-1}U \quad (57)$$

Eq.(57) can be simply written as

$$\dot{X} = A X + B U \quad (58)$$

Definitions of A and B are obvious.

Eq.(58) can be used for the time simulation. To better understand the interaction between the total body and the flexible body dynamics, steady state maneuvers (i.e. constant angular rates of the body reference frame) are studied.

By putting the derivative of ω to zero and including the aerodynamic force representation from equation (41), equation (43) becomes:

$$\begin{bmatrix} I & 0 & 0 & 0 \\ \frac{-\rho V}{2}B_{Z0} & M' & \frac{-\rho V}{2}B_{Z1} & \frac{-\rho V}{2}B_{Z2} \\ 0 & 0 & I & 0 \\ 0 & 0 & 0 & I \end{bmatrix} \begin{Bmatrix} \dot{\eta}_1 \\ \dot{\eta}_2 \\ \dot{\eta}_3 \\ \dot{\eta}_4 \end{Bmatrix} + \begin{bmatrix} 0 & -I & 0 & 0 \\ K'+A'\frac{-\rho V^2}{2}B_{T0} & G'+D' & \frac{-\rho V^2}{2}B_{T1} & \frac{-\rho V^2}{2}B_{T2} \\ 0 & -I & \beta_1 & 0 \\ 0 & -I & 0 & \beta_2 \end{bmatrix} \begin{Bmatrix} \eta_1 \\ \eta_2 \\ \eta_3 \\ \eta_4 \end{Bmatrix} = \begin{Bmatrix} 0 \\ 0 \\ 0 \\ 0 \end{Bmatrix} \quad (59)$$

Note that the coefficient matrices on LHS of the equation (59) are time invariant when the angular rate, ω, is constant. Hence the eigenvalues of the system can be used to check the stability of the system and to study the effects on modes of the system at different angular rates.

6. APPLICATION TO FINITE ELEMENT MODEL

A large-order finite element model (FEM) of a generic fighter was obtained for use in the application of this method. The aircraft planform is similar to an F/A-18, although stiffness and mass data do not necessarily represent this airplane. Although the FEM consists primarily of beam elements, it is a highly detailed model containing an A-set of 228 degrees of freedom (DOF) and approximately 200 structural elements. Aerodynamic modeling of the aircraft consisted of 230 boxes, and can be seen in Figure 2. The doublet lattice method was used to formulate aerodynamic influence coefficient matrices. Eight values of reduced frequency were used to calculate unsteady aerodynamic matrices.

Certain assumptions used to develop the equations required that some modifications be made to the model. The equations assume that the mathematical model has six DOF for every subbody. If these matrices are generated from a FEM, this is rarely true. In NASTRAN , this corresponds to the initial global set (G-set) of coordinates. These DOF cannot normally be used, however, because many are constrained due to the method of modeling and imposition of boundary conditions.

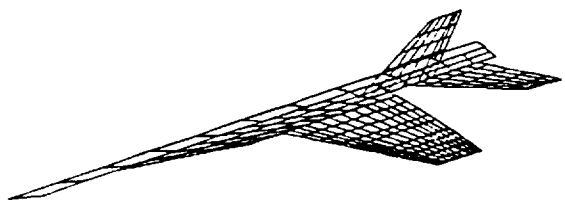

Figure 2. Aerodynamic Configuration

Table 3. Flexible Mode Frequency and Damping for Roll Rate Maneuvers
Full Stiffness

MSC/NASTRAN FLUTTER ANALYSIS		FLXAIR ANALYSIS 0.0 DEG/SEC ROLL RATE		FLXAIR ANALYSIS 90.0 DEG/SEC ROLL RATE		FLXAIR ANALYSIS 180.0 DEG/SEC ROLL RATE		FLXAIR ANALYSIS 240.0 DEG/SEC ROLL RATE	
FREQUENCY Hz	DAMPING	FREQUENCY Hz	DAMPING	FREQUENCY Hz	DAMPING	FREQUENCY Hz	DAMPING	FREQUENCY Hz	DAMPING
6.734	-.0689	6.699	-.0653	6.696	-.0653	6.685	-.0655	6.673	-.0656
8.948	-.000459	8.957	-.000422	8.955	-.000467	8.946	-.000539	8.936	-.000602
9.085	-.0740	9.056	-.0722	9.053	-.0722	9.044	-.0722	9.035	-.0722
14.192	-0.175	14.371	-0.142	14.368	-0.142	14.361	-0.142	14.353	-0.142
16.434	-.0730	16.779	-.0806	16.778	-.0806	16.774	-.0806	16.771	-.0805
18.736	-.0249	18.756	-.0297	18.755	-.0298	18.753	-.0298	18.751	-.0298
21.172	-.0188	21.812	-.0157	21.813	-.0159	21.814	-.0165	21.815	-.0162
23.172	-.0268	23.333	-.0292	23.333	-.0293	23.331	-.0294	23.333	-.0294
24.352	-.0406	24.692	-.0416	24.691	-.0416	24.689	-.0416	24.688	-.0416
29.578	-.00707	29.719	-.00878	29.276	-.00871	29.721	-.00865	29.722	-.00863
32.916	-.0458	33.439	-.0387	33.448	-.0387	33.437	-.0387	33.436	-.0387

These constrained DOF present a problem which requires either the modification of the equations or of the input matrices.

Another assumption made in the equations is that the mass matrix is block diagonal. However, the typical mass matrix from a FEM analysis contains coupling terms. These arise because of the following reasons:

1) Mass data may be input at locations other than structural grid point locations.
2) Coupling results from the use of dependency relations (multi-point constraints in NASTRAN).
3) Coupling results from the static reduction if inertia is lumped on any of the omitted DOF (Guyan reduction).

These considerations make it necessary to adjust the model as follows:

1) The inertia is relumped so that it is located at exact grid point locations.
2) Inertia at dependent DOF is relumped so that it is associated only with independent DOF.
3) Inertia located at DOF which are eliminated by the Guyan reduction process must be relumped at retained DOF (A-set).
4) A Boolean transformation matrix is formed for use in expansion of the FEM A-set DOF to the 6n DOF required by the equations. After forming the state space equations, this same matrix can be used to eliminate those DOF.

A NASTRAN flutter analysis of the vehicle was conducted for a case representing Mach .7 and an altitude of 20,000 ft. Mass, stiffness, and aerodynamic matrix data were obtained from NASTRAN for this case. The necessary matrices for the rational function approximation of the aerodynamics were obtained by a least squares fit using aerodynamic matrices for reduced frequencies of 0.0, 0.2, and 0.8 . The state space equations were formed and eigenvalue solutions were obtained for various values of roll rate.

For zero roll rate, the results agreed with the NASTRAN analysis. Increasing roll rate showed little effect on the flexible modes of the system, as can be seen in Table 3. The rigid body modes were affected, however. A root locus plot of the rigid body roots as a function of roll rate is shown in Figure 3. For zero roll rate, two stable real roots and one stable complex conjugate pair are obtained - corresponding to a roll convergence mode, a spiral mode, and an oscillatory dutch roll mode. With increasing roll rate, however, we see

Figure 3. Rigid Body Eigenvalues for Roll Rate Maneuvers Full Stiffness

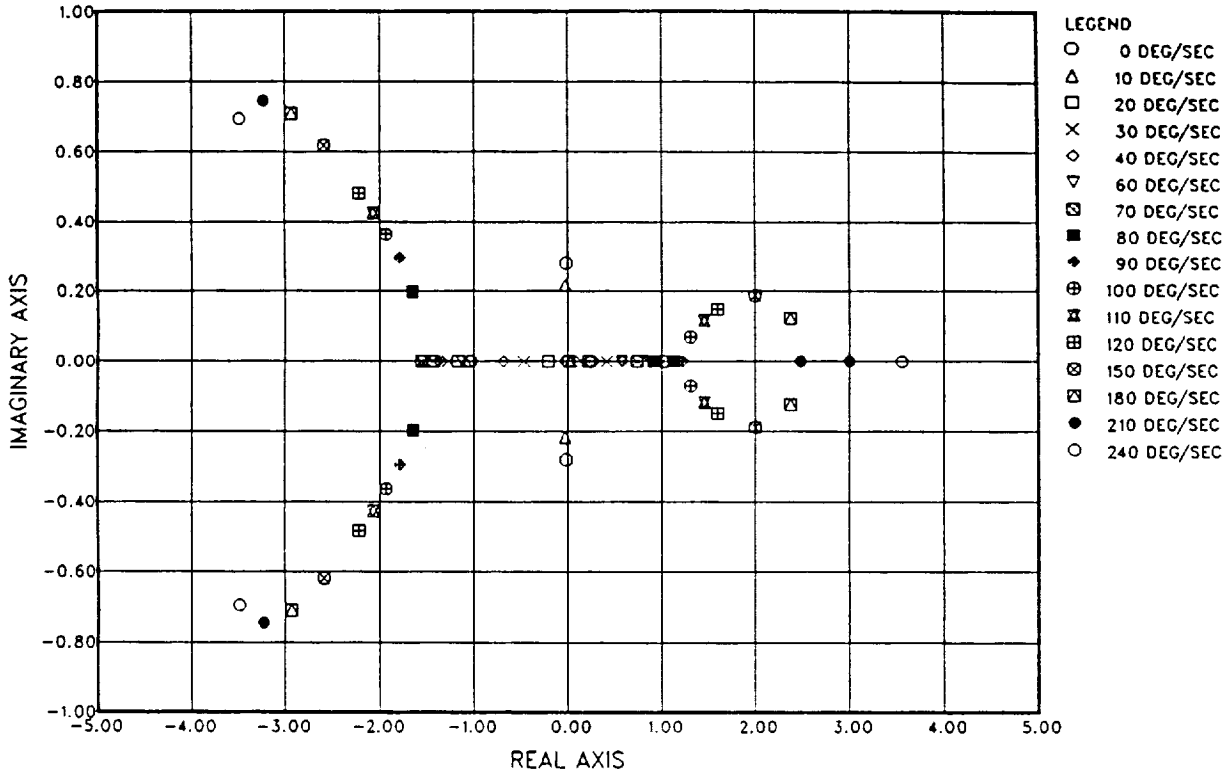

that some roots become unstable, and also change from real to complex and back again to real. Another case, representing a more flexible airplane, shows the same behavior (Figure 4), although the changes occur at lower roll rates. This case represents 50% of the initial overall airplane stiffness. Table 4 shows again that the flexible modes were not greatly affected, even for the reduced stiffness case.

7. DISCUSSION

Dynamic equations have been derived for a flexible fixed wing aircraft, including an explicit representation of unsteady aerodynamic forces. The aircraft is assumed to be a collection of elastically interconnected discrete rigid subbodies. Deformations are assumed to be small in the body reference frame, thus allowing the equations to be linearized in the deformation variables.

The hybrid coordinate method is used to derive the total body and the elemental body dynamic equations which are then converted to matrix form. These equations are integrated in a state space format, along with a rational function approximation of the unsteady aerodynamic forces. These equations can be used for simulation. For the case of constant angular velocities of the body reference frame, the coefficient matrices become time invariant, allowing the use of an eigenvalue analysis to evaluate the effects of the angular rates on the system dynamic properties. When this method is applied to a realistic finite element model of a generic high-performance fighter, significant changes in the stability characteristics of the aircraft are observed. With increasing roll rate, some roots become unstable, and also change back and forth from complex to real. The dutch roll mode becomes two real roots, one of which combines with the spiral mode to produce an unstable oscillatory mode. The other real root from the original dutch roll mode

Table 4. Flexible Mode Frequency and Damping for Roll Rate Maneuvers
50 Percent Stiffness

FLXAIR ANALYSIS 0.0 DEG/SEC ROLL RATE		FLXAIR ANALYSIS 60.0 DEG/SEC ROLL RATE		FLXAIR ANALYSIS 90.0 DEG/SEC ROLL RATE		FLXAIR ANALYSIS 180.0 DEG/SEC ROLL RATE	
FREQUENCY Hz	DAMPING	FREQUENCY Hz	DAMPING	FREQUENCY Hz	DAMPING	FREQUENCY Hz	DAMPING
4.860	-.07367	4.858	-.0737	4.855	-.0737	4.839	-.0739
6.335	-.000492	6.333	-.000553	6.331	-.000590	6.318	-.000727
6.500	-.0929	6.500	-.0930	6.500	-.0930	6.484	-.0930
10.230	-0.186	10.229	-0.186	10.227	-0.186	10.216	-0.185
11.871	-.0873	11.871	-.0874	11.870	-.0874	11.867	-.0873
13.334	-.0431	13.334	-.0431	13.333	-.0432	13.331	-.0431
15.435	-.0196	15.435	-.0199	15.435	-.0200	15.436	-.0204
16.527	-.0364	16.527	-.0365	16.527	-.0366	16.525	-.0367
17.498	-.0578	17.497	-.0578	17.497	-.0578	17.494	-.0578
21.021	-.0125	21.021	-.0124	21.022	-.0124	21.024	-.0122
23.671	-.0479	23.711	-.0479	23.671	-.0479	23.669	-.0479

Figure 4. Rigid Body Eigenvalues for Roll Rate Maneuvers
50 Percent Stiffness

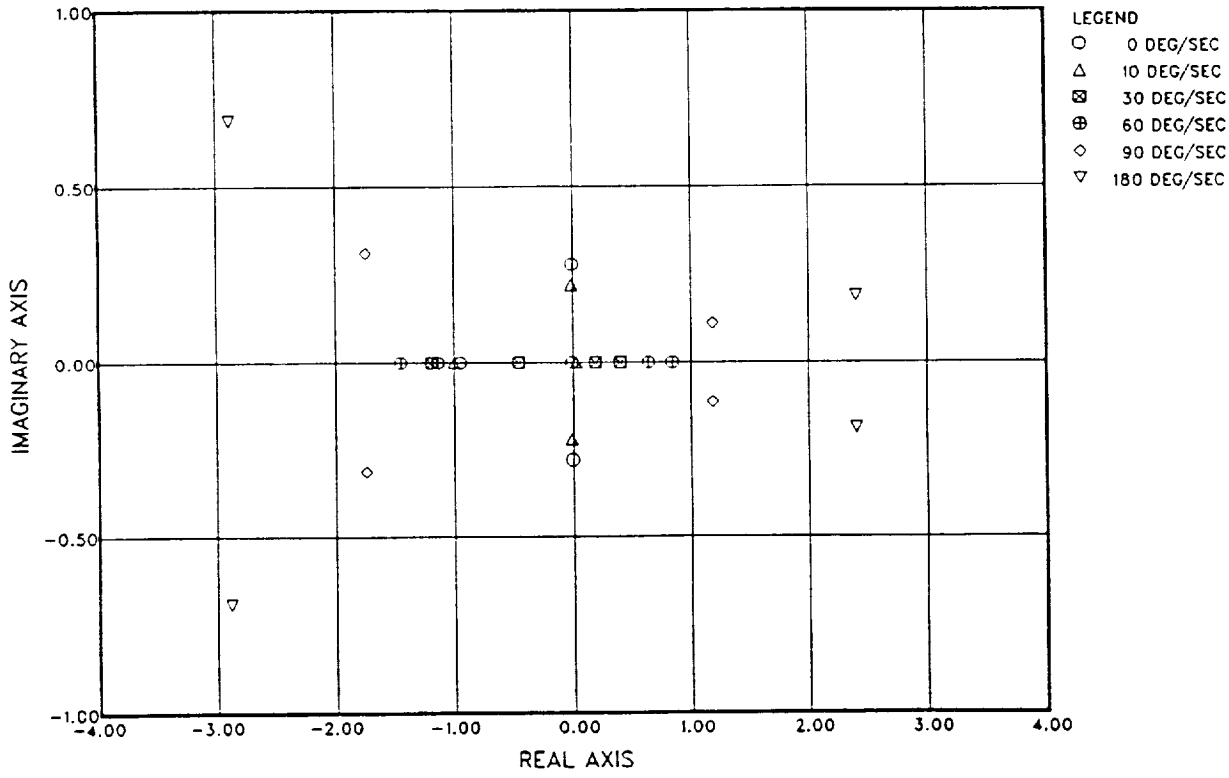

combines with the roll convergence to form another oscillatory mode which becomes more stable with increasing roll rate. The effect on the flexible modes of the aircraft was minimal for this configuration. The behavior of the rigid body modes is somewhat dependent on airframe stiffness, as can be observed for the 50% stiffness case.

It is expected that a design with increased span would show a greater effect due to roll rate for both the rigid body and flexible modes. This should be given consideration in the design of any future high-performance aircraft.

REFERENCES

[1] Meirovitch, L. and Quinn, R.D., "Equations of Motion for Maneuvering Flexible Spacecraft," Journal of Guidance, Control, and Dynamics, Vol. 10, Sept.-Oct. 1987, pp. 453-465.

[2] Laskin, R.A. and Likins, P.W., "Dynamical Equations of a Free-Free Beam Subject to Large Overall Motions," Proceedings of AAS/AIAA Astrodynamics Specialist Conference, Lake Tahoe, Nevada, Aug. 1981, paper 81-119

[3] Kane, T.R. and Levinson, D.A., "Formulation of Equations of Motion for Complex Spacecraft," Journal of Guidance and Control, Vol. 3, Mar.-Apr. 1980, pp. 99-112.

[4] Kane, T.R. and Levinson, D.A., "Large Motions of Unrestrained Space Trusses," The Journal of the Astronautical Sciences, Vol. XXVIII, Jan.-Mar., 1980, pp. 49-88.

[5] Likins, P.W., "Dynamics and Control of Flexible Space Vehicles," Jet Propulsion Laboratory, Pasadena, California, Technical Report 32-1329, Revision 1, Jan. 15, 1970.

[6] Likins, P.W., "Finite Element Appendage Equations for Hybrid Coordinate Dynamic Analysis," Jet Propulsion Laboratory, Pasadena, California, Technical Report 32-1525, Oct. 15, 1971.

[7] H.M. Youssef, A.P. Nayak, K.G. Gousman, "Integrated Total and Flexible Body Dynamics of Fixed Wing Aircraft," AIAA paper No. 88-2364 presented at 29th SDM Conference, Williamsburg, Virginia, April 18-20,1988.

[8] Roger, K. L., " Airplane Math Modeling Methods for Active Control Design," in AGARD Structures and Materials Panel, 44th Meeting, Lisbon, Portugal, April 1977.